

Nitrosopumilus adriaticus sp. nov. and *Nitrosopumilus piranensis* sp. nov., two ammonia-oxidizing archaea from the Adriatic Sea and members of the class *Nitrososphaeria*

Barbara Bayer,^{1,*} Jana Vojvoda,¹ Thomas Reinthaler,¹ Carolina Reyes,² Maria Pinto¹ and Gerhard J. Herndl^{1,3}

Abstract

Two mesophilic, neutrophilic and aerobic marine ammonia-oxidizing archaea, designated strains NF5^T and D3C^T, were isolated from coastal surface water of the Northern Adriatic Sea. Cells were straight small rods 0.20–0.25 µm wide and 0.49–2.00 µm long. Strain NF5^T possessed archaella as cell appendages. Glycerol dibiphytanyl glycerol tetraethers with zero to four cyclopentane moieties (GDGT-0 to GDGT-4) and crenarchaeol were the major core lipids. Menaquinone MK_{6:0} was the major respiratory quinone. Both isolates gained energy by oxidizing ammonia (NH₃) to nitrite (NO₂⁻) and used bicarbonate as a carbon source. Strain D3C^T was able to use urea as a source of ammonia for energy production and growth. Addition of hydrogen peroxide (H₂O₂) scavengers (catalase or α-keto acids) was required to sustain growth. Optimal growth occurred between 30 and 32 °C, pH 7.1 and 7.3 and between 34 and 37‰ salinity. The cellular metal abundance ranking of both strains was Fe>Zn>Cu>Mn>Co. The genomes of strains NF5^T and D3C^T have a DNA G+C content of 33.4 and 33.8 mol%, respectively. Phylogenetic analyses of 16S rRNA gene sequences revealed that both strains are affiliated with the class *Nitrososphaeria*, sharing ~85 % 16S rRNA gene sequence identity with *Nitrososphaera viennensis* EN76^T. The two isolates are separated by phenotypic and genotypic characteristics and are assigned to distinct species within the genus *Nitrosopumilus* gen. nov. according to average nucleotide identity thresholds of their closed genomes. Isolates NF5^T (=JCM 32270^T =NCIMB 15114^T) and D3C^T (=JCM 32271^T =DSM 106147^T =NCIMB 15115^T) are type strains of the species *Nitrosopumilus adriaticus* sp. nov. and *Nitrosopumilus piranensis* sp. nov., respectively.

INTRODUCTION

Ammonia-oxidizing archaea (AOA) are among the most ubiquitous and abundant microorganisms on Earth [1, 2]. They are especially abundant in deep waters of the global ocean where they represent 20–40 % of the prokaryotic community [3, 4]. AOA perform the first and rate-limiting step of nitrification, oxidizing ammonia (NH₃) into nitrite (NO₂⁻), thereby generating energy for autotrophic growth [5, 6]. Hence, they represent key players in the global cycling of nitrogen and carbon [7, 8]. AOA typically thrive under conditions where nutrients are extremely limited, exhibiting a remarkably high affinity for ammonia [9, 10]. In addition to predominating in oxygenated waters, marine AOA are abundant and active in oxygen minimum zones (OMZs) [11–13], being able to grow under suboxic (<10 µM

O₂) conditions [14]. AOA have also been identified as major contributors of the greenhouse gas nitrous oxide (N₂O) [15], particularly in OMZs [16]. Future increases in ocean deoxygenation could potentially influence N₂O production by archaeal ammonia oxidation [17, 18]. Thus, understanding their physiology is of great importance to predict future ocean scenarios, particularly in the light of global change.

The first AOA culture, *Nitrosopumilus maritimus* SCM1^T, was obtained from a tropical marine aquarium [6], additional strains were isolated or enriched from marine and estuarine environments [18–24], neutral and acidic soils [25–28], coal-tar contaminated sediment [29], hot springs [30–34], wastewater treatment plants [35, 36] and an aquarium biofilter [37]. All cultured representatives are autotrophic ammonia oxidizers, but vary in their capability

Author affiliations: ¹Department of Limnology and Bio-Oceanography, Center of Functional Ecology, University of Vienna, Vienna, Austria; ²Department of Environmental Geosciences, Environmental Science Research Network, University of Vienna, Vienna, Austria; ³Department of Marine Microbiology and Biogeochemistry, NIOZ Royal Netherlands Institute for Sea Research, Utrecht University, Den Burg, The Netherlands.

***Correspondence:** Barbara Bayer, barbara.bayer@outlook.com

Keywords: ammonia-oxidizing archaea; *Nitrosopumilus*; *Nitrosopumilaceae*; elemental composition; nitrification inhibitors.

Abbreviations: ANI, average nucleotide identity; AOA, ammonia-oxidizing archaea; AOB, ammonia-oxidizing bacteria; DIC, dissolved inorganic carbon; GDGT, glycerol dibiphytanyl glycerol tetraether; MK, menaquinone; OMZ, oxygen minimum zone.

The GenBank/EMBL/DDBJ accession numbers for the genomes of strains NF5^T and D3C^T are CP011070 and CP010868, respectively. 16S rRNA sequences are deposited under the accession numbers MK139955 and MK139956.

Three supplementary figures and four supplementary tables are available in the online version of this article.

to use alternative substrates such as urea [19, 25, 28, 29, 31, 36, 38, 39] or cyanate [40]. Some strains have also been described to require small additions of organic acids [25, 38]. However, this apparent necessity has recently been attributed to their sensitivity towards hydrogen peroxide (H_2O_2), which is detoxified by alpha-ketoacids [41]. Hence, these requirements can be overcome with the addition of the H_2O_2 -detoxifying enzyme catalase or the presence of co-cultured heterotrophic catalase-positive bacteria ([41] and Bayer et al., under review). Despite their broad distribution in various different environments, all sequenced AOA to date share common genomic features. These include copper-based enzymes for ammonia oxidation and electron transfer, a variant of the autotrophic 3-hydroxypropionate/4-hydroxybutyrate (HP/HB) cycle for carbon fixation, and synthesis pathways for various B vitamins including cobalamin (vitamin B12) [23, 30, 42, 43].

Here, we report the formal taxonomic description of two closely related isolates from coastal surface waters of the Northern Adriatic Sea, strains NF5^T and D3C^T. We extend the original characterization of ‘*Candidatus Nitrosopumilus adriaticus*’ NF5 and ‘*Candidatus Nitrosopumilus piranensis*’ D3C [19], including the first measurements of cellular elemental composition of AOA. We formally describe *Nitrosopumilus adriaticus* sp. nov. and *Nitrosopumilus piranensis* sp. nov., two novel species of the genus *Nitrosopumilus* [18] within the family *Nitrosopumilaceae* of the class *Nitrososphaeria* [44].

METHODS

Sample source and culture conditions

Seawater was collected in the Northern Adriatic Sea at approximately 0.5 m depth off the coast of Piran, Slovenia (45.518° N, 13.568° E) in two consecutive months (November 2011: strain NF5^T; December 2011: strain D3C^T). At the time of sampling, seawater temperatures ranged between 13.1 and 15.5 °C, and ammonium concentrations varied between 0.12 and 0.48 μM. Enrichment cultures were initiated as previously described [19]. Cultures were grown in SCM medium and maintained in 30 ml polypropylene bottles at 30 °C in the dark without shaking. Axenic cultures were established by adding erythromycin (25 μg ml⁻¹) in addition to purified catalase (5 U ml⁻¹). Ammonia oxidation activity was monitored by measuring $\text{NH}_3/\text{NH}_4^+$ consumption and NO_2^- production using the orthophthalaldehyde (OPA) [45] and Griess [46] reagents, respectively. Growth was measured by flow cytometry as previously described [47]. Subsequent sub-culturing was performed by inoculating fresh medium (2.5–5 % v/v inoculum) with cells in mid-exponential phase, which corresponded to a residual $\text{NH}_3/\text{NH}_4^+$ concentration of approximately 300 μM.

Physiological characterization and ammonia oxidation inhibitors

Utilization of urea as an alternative substrate as well as temperature and pH optima for both strains were previously

determined [19]. Salinity optima were determined by maintaining optimum temperature and pH. Varying salinities were established by adjusting NaCl concentrations to 5–70 ‰ in 3–5 ‰ intervals (w/v) in duplicate cultures. Samples were taken every 3–5 days and NO_2^- production was measured as described above. The effect of two ammonia oxidation inhibitors, 2-phenyl-4,4,5,5-tetramethylimidazoline-1-oxyl 3-oxide (PTIO, Sigma P5084) and 2-(4-carboxyphenyl)-4,4,5,5-tetramethylimidazoline-1-oxyl 3-oxide (carboxy-PTIO, Sigma C221) was tested on both strains. To duplicate cultures, 100 μM PTIO or carboxy-PTIO were added and ammonium concentrations were measured every 2–3 days as described above.

Leucine incorporation and DIC fixation

Leucine incorporation was measured by incubating 5 ml aliquots with a final concentration of 50 nM [³H]-leucine (specific activity 4.44×10^9 Bq mmol⁻¹, American Radiolabeled Chemicals). Duplicate live samples and one formaldehyde-killed blank were incubated in a water bath in the dark at 30 °C for 24 h. Incubations were terminated by adding formaldehyde (2 % final concentration) to the live samples. Samples and blanks were filtered through 0.2 μm polycarbonate filters (Millipore, 25 mm filter diameter) supported by cellulose acetate filters (Millipore, HAWP, 0.45 μm pore size) on a filtration manifold (Millipore). On the manifold, the filters were rinsed twice with 5 % ice-cold trichloroacetic acid to precipitate proteins. Subsequently filters were dried in 20 ml scintillation vials, 8 ml of scintillation cocktail (FilterCount, Perkin Elmer) was added, and after 18 h the vials were counted on a scintillation counter (Tri-Carb 2100TR, Perkin Elmer). The instrument was calibrated with internal and external standards. To compare leucine incorporation rates of NH_3 -replete and NH_3 -starved cells, cultures in late exponential growth phase were transferred at 20 % (v/v) inoculum into fresh medium with or without 1 mM NH_4Cl , and leucine incorporation was measured after 3 days of incubation.

Dissolved inorganic carbon (DIC) fixation was measured via the incorporation of [¹⁴C]-bicarbonate as described by Herndl et al. [48] with modifications. [¹⁴C]-bicarbonate (specific activity 1.85×10^9 Bq, American Radiolabeled Chemicals) was added to 5 ml duplicate live samples and one formaldehyde-fixed blank. The live samples and the blank were incubated in the dark at 30 °C in a water bath for 24 h. Incubations were terminated by adding formaldehyde (2 % v/v) to the samples, filtered onto 0.2 μm polycarbonate filters and rinsed with 10 ml of artificial seawater. Subsequently, the filters were placed in a desiccator in fumes of concentrated HCl (37 %) for 12 h to remove excess [¹⁴C]-bicarbonate. The filters were transferred to scintillation vials, 8 ml of scintillation cocktail (FilterCount, Perkin Elmer) was added, and after 18 h the disintegrations per minute (DPM) counted in the scintillation counter for 10 min. The resulting mean DPM of the samples were corrected for the DPM of the blank, converted into organic

Table 1. Major characteristics of strains NF5^T and D3C^T compared to those of other *Nitrosopumilus* species

All data for *Nitrosopumilus maritimus* SCM1^T, *Nitrosopumilus cobalaminigenes* HCA1^T, *Nitrosopumilus oxycloinae* HCE1^T and *Nitrosopumilus ureiphilus* PS01^T were previously reported by Qin et al. [18]. ND, No data; –, negative; +, positive.

Characteristic	NF5 ^T	D3C ^T	SCM1 ^T	HCA1 ^T	HCE1 ^T	PS01 ^T
Growth temperature (°C):						
Range	15–34	15–37	15–35	10–30	4–30	10–30
Optimum	30–32	32	32	25	25	26
Growth pH:						
Range	6.8–8.0	6.8–8.0	6.8–8.1	6.8–8.1	6.4–7.8	5.9–8.1
Optimum	7.1	7.1–7.3	7.3	7.3	7.3	6.8
Salinity (‰):						
Range	10–55	15–65	16–55	15–40	10–40	15–40
Optimum	34	37	32–37	32	25–32	25
Maximum ammonia oxidation (fmol cell ⁻¹ d ⁻¹)	9.6	10.9	12.7	6.0	5.8	2.9
Average ammonia oxidation (fmol cell ⁻¹ d ⁻¹)*	6.5±3.2	7.2±3.7	ND	ND	ND	ND
Average carbon fixation (fmol cell ⁻¹ d ⁻¹)*	0.69±0.29	0.64±0.37	ND	ND	ND	ND
Minimum generation time (h)	34	27	19	30	33	54
Ammonium tolerance (mM)	25†	30	10	10	1	20
Nitrite tolerance (mM)	15‡	10‡	2	ND	ND	ND
Use of urea	–	+	–	–	–	+
Flagellum	+	–	–	–	–	+§
DNA G+C content (mol%)	33.4	33.8	34.2	33	33.1	33.4

*Average and standard deviation are shown.

†~900 µM NH₄⁺ was oxidized after approx. 1 month incubation.

‡~800 µM NH₄⁺ was oxidized after approx. 2 months incubation.

§Based on the presence of archaeella genes in the genome.

carbon fixed over time and corrected for the DIC concentration in the medium.

DIC uptake rates were calculated using the following formula:

$(\text{DPMs} - \text{DPMb}) \times \text{DICw} / (\text{DPMtr} \times \text{inc. time})$ where DPM are the disintegrations per minute measured in the

scintillation counter, for the sample (s) and the blank (b). DICw denotes the dissolved inorganic carbon concentration in seawater, DPM tracer (tr) is the calculated DPMs for the [¹⁴C]-bicarbonate added to the incubations.

Cellular carbon content was estimated from DIC incorporation rates divided by the number of newly produced cells over time averaged over 7 days.

Cellular metal concentrations and C : N ratios

Cultures were grown in 1L Schott flasks as described above, and cells were harvested in the late exponential growth phase by centrifugation (20 000 *g* at 10 °C for 1.5 h). Cell pellets were washed three times (see different washing procedures below) and transferred into nitric acid-washed 1.5 ml tubes. The following washing procedures were applied to distinguish between intracellular and total metal concentrations: (1) three washes with synthetic seawater (Paragon Scientific Ld) diluted to 50 % with Milli-Q water (v/v), (2) one wash with an oxalate-EDTA solution in 50 % synthetic seawater (v/v) modified from Tovar-Sanchez et al. [49] (final conc.: 10 mM EDTA, 10 mM sodium citrate, 25 mM oxalic acid, pH was adjusted to 7.5) including a 5 min incubation step and two subsequent washes with synthetic seawater, (3) one wash with 0.5 mM EDTA and one wash with 0.5 mM TETA each including 5 min incubation time, and one subsequent wash with synthetic seawater.

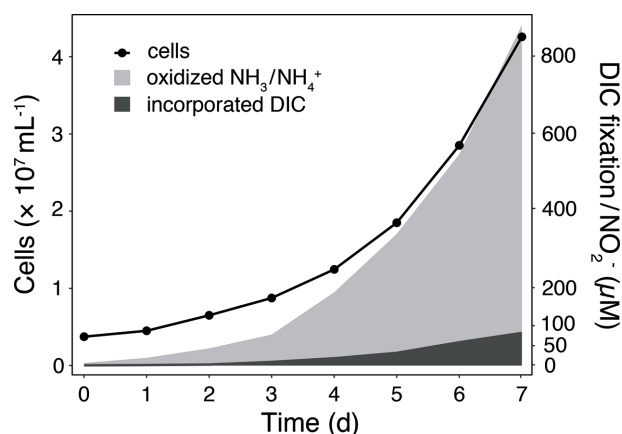


Fig. 1. Relationship between cell growth, ammonia oxidation (light grey) and DIC fixation (dark grey) of strain NF5^T.

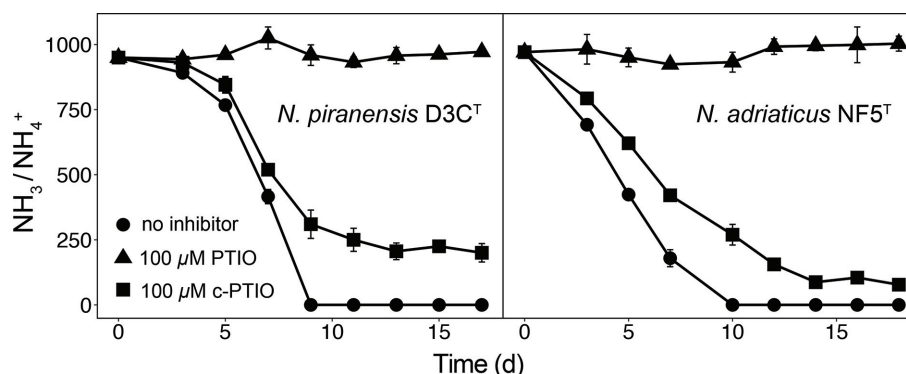


Fig. 2. Ammonia consumption of strains D3C^T (left) and NF5^T (right) after additions of the ammonia oxidation inhibitors PTIO (triangles) and carboxy-PTIO (squares) in comparison to control incubations without inhibitors (circles). Error bars represent the range of the mean from measurements of duplicate cultures.

TETA [1,4,8,11-tetraazacyclotetradecane 1,4,8,11-tetraacetic acid hydrochloride hydrate] is a chelator with selective affinity for Cu²⁺ [50]. Each wash was performed with 1 ml washing solution and was followed by centrifugation (20 000 g, 4 °C) for 20 min. Cell pellets were subsequently digested by adding 500 μl of 70 % trace metal grade nitric acid (Fisher Scientific) and 500 μl 30 % hydrogen peroxide (Sigma) and incubated at 70 °C for 6 h. The digest was diluted with 5 ml Milli-Q water and filtered through 0.45 μm cellulose acetate syringe filters (Sartorius). Metal concentrations were determined using an inductively coupled plasma-mass spectrometer (ICP-MS; Agilent 7700). Due to the long generation times and low biomass production, 1L culture was required for a single measurement, and it was not feasible to run biological replicates.

To determine cellular C:N ratios, 1L of culture was harvested as described above, pellets were washed three times with medium devoid of HEPES buffer, NaHCO₃ and NH₄Cl to exclude sources of carbon and nitrogen. Pellets were subsequently dried for 1 h (Concentrator Plus, Eppendorf) and measured on a CHNS elemental analyser (Vario MICRO cube, Elementar).

Cell cryopreservation and resuscitation

Cultures were grown in SCM medium with addition of catalase as described above. When cultures reached late exponential growth (cell abundance >10⁷ cells ml⁻¹), 1 ml of culture was transferred to 2 ml cryovials (Biozym) and 100 % DMSO (Sigma D2650) was added to a final concentration of 3–4 % (v/v). Tubes were carefully inverted three times, incubated at room temperature for 5 min and subsequently stored at –80 °C. To resuscitate the cultures, vials were defrosted in a water bath at 37 °C for 1–2 min, and the entire contents were immediately transferred into 19 ml fresh, pre-warmed SCM medium. After cryopreservation, longer lag phases of up to 2 weeks were observed. Successful resurrection after storage for up to 1.5 years has been tested.

Electron microscopy and lipid analysis

Scanning and transmission electron microscopy analyses have been performed previously and are described in Bayer et al. [19]. Core lipids and intact polar lipids were analysed previously and described by Elling et al. [51].

Table 2. Elemental composition and cellular metal concentrations of strains NF5^T and D3C^T. Carbon and nitrogen concentrations are given in fg cell⁻¹, metal concentrations are given in amol cell⁻¹ and C:N ratios are given in mol C: mol N

Ni concentrations were in a similar range as Co concentrations, however, these values were omitted due to variable Ni contamination in blanks.

Strain*	C	N	C:N	Fe	Zn	Cu	Mn	Co
NF5 ^T (1)	16.65±7.5†	ND	3.91‡	1.140	0.192	0.110	0.046	0.0028
D3C ^T (1)	16.30‡	4.78‡	3.98‡	1.030	0.222	0.127	0.058	0.0034
D3C ^T (2)	ND	ND	ND	0.863	0.209	0.095	0.050	0.0025
D3C ^T (3)	ND	ND	ND	0.720	0.167	0.086	0.040	0.0019

*Treatments (1, 2 and 3) are described in the Material and Methods section. Treatment (1) results in total cellular metal concentrations whereas treatments (2) and (3) results in intracellular metal concentrations.

†Derived from DIC incorporation rates, average and standard deviation is shown.

‡Derived from elemental analyser measurements.

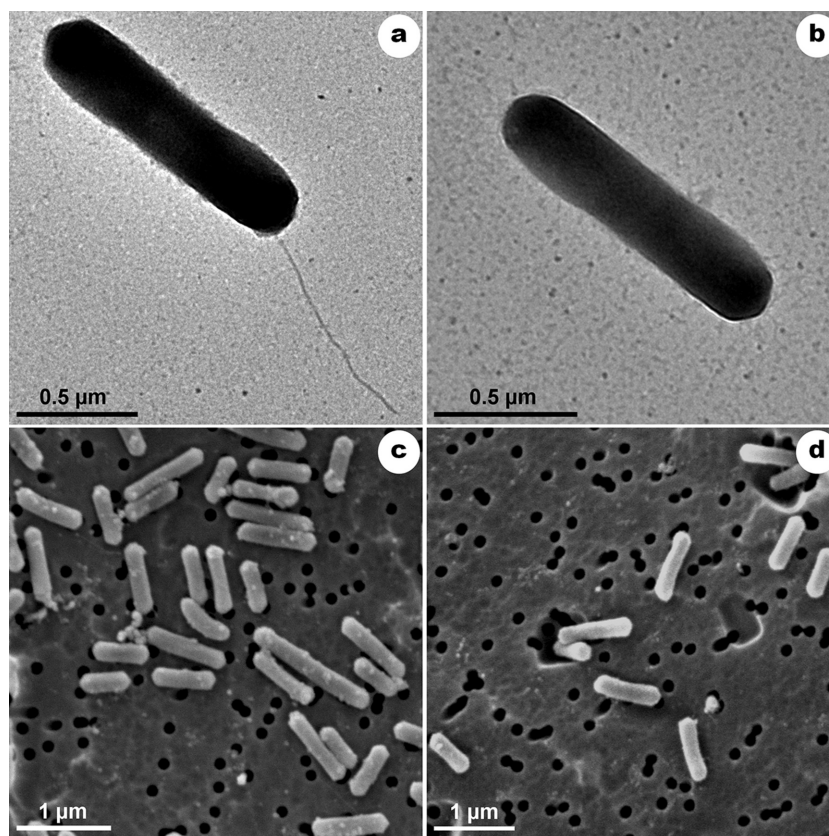


Fig. 3. Transmission electron microscopy (a, b) and scanning electron microscopy (c, d) images of strains NF5^T (left) and D3C^T (right). This figure has previously been published by Bayer et al. [19] under a Attribution 4.0 International (CC BY 4.0) License.

Phylogenetic analyses

Full length 16S rRNA gene sequences from AOA isolates and enrichment cultures were retrieved from the National Centre for Biotechnology Information (NCBI) and aligned with the multiple sequence alignment software MAFFT (FFT-NS-i method) [52]. Unreliable sequence positions were automatically trimmed with the software BGME (Block Mapping and Gathering with Entropy) using standard settings [53]. A phylogenetic tree was calculated by using the maximum-likelihood method with the software IQ-Tree, based on the best-fit model of nucleotide substitution (selected model: GTR+F+G4) [54]. The ultrafast bootstrap (UFBoot) and SH-aLRT feature options were used to generate support values from 1000 replicates.

RESULTS AND DISCUSSION

Physiology and ecology

Strains NF5^T and D3C^T are mesophilic and neutrophilic organisms, growing optimally at 30–32 °C and pH 7.1–7.3 (Table 1). They produce energy by oxidizing ammonia aerobically to nitrite at stoichiometric levels [19]. The minimum generation time of strains NF5^T and D3C^T was 34 h and 27 h, respectively, and growth was impaired by agitation, as

observed for *N. maritimus* SCM1^T [6]. Strain D3C^T grew equally well with urea or ammonia as an energy source [19]. While the ability to use urea in general appears to be widespread among AOA, it is not shared by phylogenetically closely related marine strains, indicating niche partitioning [19, 38, 39]. Strains NF5^T and D3C^T were able to grow at a broader salinity range than the other four described *Nitrosopumilus* species (Table 1). However, growth of strain D3C^T with salt concentrations of 65‰ was only observed after more than 1 month of incubation (Fig. S1b, available in the online version of this article), suggesting that comparisons between studies might be difficult if incubation times vary. Similarly, strains NF5^T and D3C^T were completely inhibited at considerably higher ammonia and nitrite concentrations than previously described for other species (Table 1), but inhibitory effects at high concentrations of ammonia and nitrite (i.e., up to 30 and 15 mM, respectively, for strain D3C^T) could only be overcome if incubated for >2 months. A lower tolerance against high ammonia concentrations with increasing pH (inhibition at 2 mM and 0.3 mM of NH₄⁺/NH₃ at pH 7.6 and 8.2, respectively) has previously been observed for strain SCM1^T [55]. In this study, the pH of the growth medium was ~7.2 in contrast to ~7.5 used by Qin et al. [18], potentially explaining the higher tolerance of

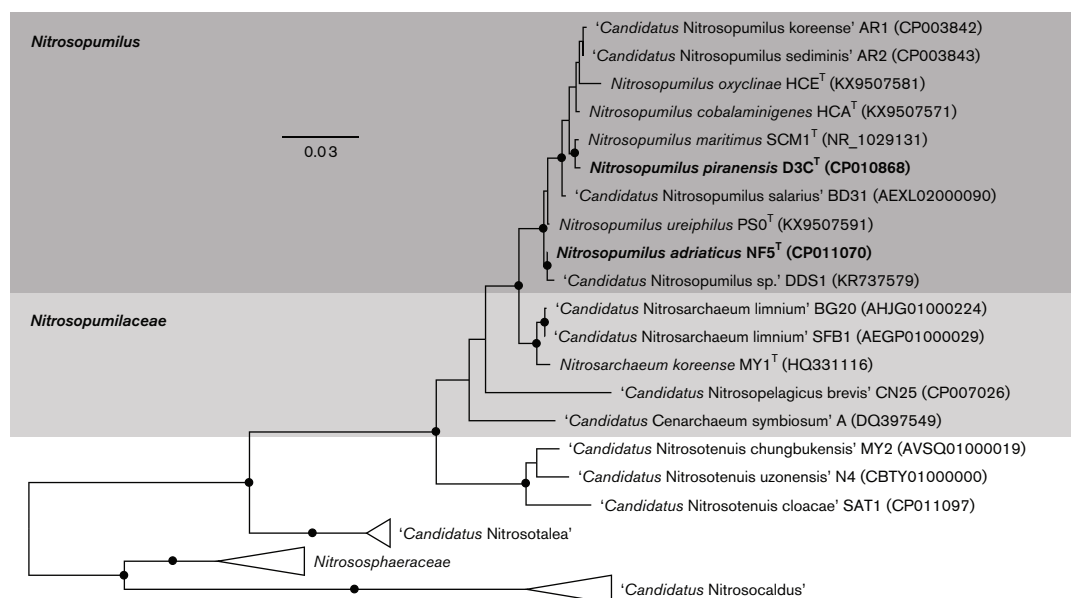


Fig. 4. Phylogenetic maximum-likelihood tree of full-length 16S rRNA gene sequences from cultivated members of the class *Nitrososphaeria* showing the affiliation of strains NF5^T and D3C^T. Support values were inferred from 1000 replicates and are represented on the respective branches by black circles (UFBoot ≥ 95 , SHaLRT ≥ 80).

strains NF5^T and D3C^T against high concentrations of ammonia. Both strains were tolerant against the antibiotics kanamycin (100 $\mu\text{g ml}^{-1}$), streptomycin (100 $\mu\text{g ml}^{-1}$), spectinomycin (100 $\mu\text{g ml}^{-1}$), carbenicillin (100 $\mu\text{g ml}^{-1}$), erythromycin (50 $\mu\text{g ml}^{-1}$) and ofloxacin (50 $\mu\text{g ml}^{-1}$), but sensitive towards chloramphenicol (25 $\mu\text{g ml}^{-1}$) and tetracycline (25 $\mu\text{g ml}^{-1}$).

Average ammonia oxidation rates of strains NF5^T and D3C^T were 6.5 (± 3.2) and 7.2 (± 3.7) fmol cell⁻¹ d⁻¹, respectively, which is within the range of estimated rates in the Eastern Tropical North Pacific Ocean (0.1–4.1 fmol cell⁻¹ d⁻¹), off the California coast (0.2–15 fmol cell⁻¹ d⁻¹) and the coastal North Sea (≤ 7 fmol cell⁻¹ d⁻¹) [5, 56, 57]. Autotrophic carbon fixation rates of strains NF5^T and D3C^T were 0.69 (± 0.29) and 0.64 (± 0.37) fmol C cell⁻¹ d⁻¹ (Table 1), being much higher than rates reported in the aphotic zone of the North Atlantic Ocean [48, 58] but within the range from less energy-limited systems (Table S1). While nitrification rates are generally lower in more oligotrophic open-ocean regions [59], the occurrence of different AOA communities in deeper water layers in contrast to *Nitrosopumilus*-dominated coastal waters [60] could potentially also explain the discrepancy between *in situ* rates and those obtained in this study. The carbon yield from nitrification (fmol C fixed cell⁻¹ d⁻¹/fmol N oxidized cell⁻¹ d⁻¹) of strains NF5^T and D3C^T was ~ 0.1 , amounting to 10 mol NH₃ oxidized for every mole of carbon fixed (Fig. 1), which is \sim two times higher than observed for AOB [61]. This apparent higher yield could potentially be explained by the presence of a more efficient carbon fixation pathway in AOA as compared to AOB [62].

The nitrification inhibitor PTIO [2-phenyl-4,4,5,5-tetramethylimidazoline-1-oxyl-3-oxide] has been reported to inhibit AOA due to its capacity to scavenge nitric oxide (NO), a proposed important intermediate in the archaeal ammonia oxidation pathway [63, 64]. Many studies used PTIO and carboxy-PTIO treatments to distinguish between archaeal and bacterial ammonia oxidation [36, 65–67]. However, comparing both inhibitors, our results show that while PTIO completely inhibited strains NF5^T and D3C^T, carboxy-PTIO had almost no effect on the ammonia oxidation activity of both strains (Fig. 2). Additionally, the heterotrophic alphaproteobacterium '*Oceanicaulis alexandrii*', the last contaminant of enrichment cultures of strains NF5^T and D3C^T [19], was also inhibited by additions of 100 μM PTIO (see Fig. S2). These results indicate that PTIO has a broad inhibitory effect, being potentially toxic to different microbes rather than representing a selective inhibitor for AOA.

Growth of strains NF5^T and D3C^T was stimulated by hydrogen peroxide (H₂O₂) scavengers (i.e., catalase, alpha-keto acids; Bayer et al., *under review*), as previously observed for *N. viennensis* EN76^T and other members of the *Nitrosopumilus* genus [18]. Although AOA genomes encode for transporters suggested to play a role in the uptake of diverse classes of organic compounds [68], the addition of various organic substrates other than alpha-keto acids (i.e., pyruvate, alpha-keto glutarate, oxaloacetate) did not have a positive effect and in some cases even inhibited growth of AOA [18, 25]. While AOA-dominated archaeal communities have previously been shown to take up amino acids [4, 69], strains NF5^T and D3C^T incorporated leucine at extremely

low rates of 0.009 and 0.011 amol leucine cell⁻¹ d⁻¹, respectively (Table S1). These values are ~10–100 times lower than those reported for *Prochlorococcus*, the most abundant photoautotrophic organism in the global ocean (Table S1) [70]. Leucine incorporation of strains NF5^T and D3C^T decreased ~30–100 fold when ammonium was omitted from the medium (Table S1), indicating that neither strain was able to efficiently use leucine as a source of energy and/or carbon and only incorporated traces of leucine during high metabolic activity. However, it still remains unclear if other AOA clades exhibit alternative metabolisms, either growing mixo- or heterotrophically.

The average elemental composition of strains NF5^T and D3C^T was (C₄N₁)₁₀₀₀Fe₂Zn_{0.5}Cu_{0.25}Mn_{0.1}Co_{0.006} (Table 2), which is similar to the elemental stoichiometry of Fe-replete *Prochlorococcus* cultures ((C₄N₁)₁₀₀₀Fe_{3.3}Mn_{0.1}Zn_{0.045}Cu_{0.02}Co_{0.0026}, normalized to N from values previously reported by Cunningham *et al.* [71]). However, intracellular concentrations of Cu and Zn were one order of magnitude higher in strains NF5^T and D3C^T than reported for *Prochlorococcus* [71]. While Zn represents an important element in all three domains of life (e.g. present in RNA polymerases and alcohol dehydrogenases [72]), AOA in particular contain a large number of Cu-containing proteins likely involved in electron transfer. These include periplasmic multicopper oxidases, plastocyanins and blue copper domain-containing proteins instead of Fe-containing c-type cytochromes [43, 73]. Nevertheless, Fe was the most abundant metal in cells of strains NF5^T and D3C^T, being on average 10 times more abundant than Cu in whole cell extracts and intracellular fractions (Table 2). Indeed, a number of iron-containing proteins were identified at high relative abundance in proteomes of strains NF5^T and D3C^T (Bayer *et al.*, *under review*) and in transcriptomes of ‘*Ca. Nitrosopelagicus brevis*’ [39], suggesting an important role of iron in the cellular metabolism of AOA. In addition, the high intracellular Fe:C quotas of ~600 (μmol Fe: mol C, Table 2) suggest that AOA might store iron under replete conditions. This notion is supported by the expression of putative iron storage proteins of the ferritin/Dps domain family (Bayer *et al.*, *under review*) and observations of electron-dense particles in electron micrographs of *N. viennensis* EN76^T [44].

The factors controlling the vertical distribution of AOA in the ocean and their absence in sunlit surface waters has been a topic of debate since their discovery. Competition with phytoplankton for ammonia [74], inhibition by light or light-induced oxidative stress [75, 76] and copper bio-availability [73] have been suggested as drivers of AOA distribution patterns. However, our results indicate that the availability of metals other than copper could potentially play a more important role for marine AOA than previously assumed, in particular iron which appears to be more abundant than copper in cells of strains NF5^T and D3C^T.

Morphology and lipid composition

Both strains share very similar shape and size. They are slender, straight rods that range from 0.20 to 0.25 μm by 0.49–2.00 μm (Fig. 3), similar to previous reports on other *Nitrosopumilus* species [18]. The genome of strain NF5^T contains genes encoding archaeella (archaeal flagella) and chemotaxis proteins [19]. Cells of strain NF5^T occasionally appeared to contain appendages (7 % of cells, *n*=300) with a diameter of 11–14 nm [19] (Fig. 3), which is within the typical size range reported for archaeella [77]. Both genomes also contain genes encoding for putative pili, however, we did not observe any pili-like structures in electron microscopy.

Major core lipid types identified in strains NF5^T and D3C^T were glycerol dibiphytanyl glycerol tetraethers (GDGTs) with zero to four cyclopentane moieties (GDGT-0 to GDGT-4), hydroxylated GDGTs (OH-GDGTs), crenarchaeol (a GDGT containing four cyclopentane moieties and one cyclohexane moiety), glycerol diphytanyl diethers (archaeols), glycerol trialkyl glycerol tetraethers (GTGTs), and glycerol dialkanol diethers (GDDs) [51]. Abundances of archaeol, methoxy archaeol and crenarchaeol relative to total lipids varied between strains NF5^T and D3C^T and other mesophilic *Nitrosopumilus* strains [51], with strain NF5^T containing the highest proportions of archaeol and methoxy archaeol (4.2 and 11.5 %, respectively) (Table S2a). Elling *et al.* [51] reported on the high potential of methoxy archaeol as a diagnostic biomarker for AOA by relating total abundance of methoxy archaeol to that of the universal archaeal lipid biomarker archaeol.

The major intact polar lipids of strains NF5^T and D3C^T were GDGTs with monoglycosyl, diglycosyl, phosphohexose and hexose-phosphohexose headgroups [51] (Table S2b). Both strains synthesized menaquinones with fully unsaturated (MK_{6:0}) and monounsaturated (MK_{6:1}) side chains composed of six isoprenoid units, whereas MK_{6:0} made up the majority of detected menaquinones (93 and 89 % in strains NF5^T and D3C^T, respectively) [51]. MK_{6:0} and MK_{6:1} have been suggested as additional biomarkers for AOA, as they only constitute minor quinones in some thermophilic Crenarchaeota and Euryarchaeota and have not been detected in other cultivated mesophilic archaea [78].

Phylogeny

Strains NF5^T and D3C^T are phylogenetically located within the family *Nitrosopumilaceae* and belong to the genus *Nitrosopumilus* (Fig. 4). Members of this family have previously been assigned to the order *Nitrosopumilales* within the class *Nitrososphaeria* of the phylum Thaumarchaeota [18, 79]. Recently, a genome based taxonomy was proposed including the normalization of taxonomic ranks according to relative evolutionary divergence and the removal of polyphyletic groups [80]. On the basis of this new taxonomic proposal, the former ‘Thaumarchaeota’ are included as class *Nitrososphaeria* within the phylum Crenarchaeota and all thus far characterized AOA are included in the order *Nitrososphaerales* (<http://gtadb.ecogenomic.org>).

Within the *Nitrosopumilus* genus, different species typically share high 16S rRNA gene sequence identity. Strain NF5^T shares 99 % 16S rRNA gene sequence identity with strain D3C^T, and between 97.9 and 99.6 % with other *Nitrosopumilus* species. Both strains share ~97.5 % 16S rRNA gene sequence identity with members of the genus *Nitrosarchaeum*, and ~93.5 % with the provisional genera '*Nitrosopelagicus*' and '*Cenarchaeum*' within the *Nitrosopumilaceae* family. With the more distantly related Group 1.b AOA *Nitrososphaera viennensis* EN76^T, strains NF5^T and D3C^T share ~85 % 16S rRNA gene sequence identity. Despite their high 16S rRNA gene sequence identity, the complete genomes of strains NF5^T and D3C^T share <80 % average nucleotide identity (ANI) (Table S3). In general, ANI values between genomes of different members of the *Nitrososphaeria* class are consistent with 16S rRNA gene sequence phylogeny, with the exception of '*Ca. Cenarchaeum symbiosum*' (Fig. 4, Table S3).

The genomes of strains NF5^T and D3C^T are 1.80 and 1.71 Mb in size, respectively, representing the largest genomes reported for members of the *Nitrosopumilus* genus thus far [19]. Furthermore, both genomes encode for a larger number of proteins (2184 and 2161 in strains NF5^T and D3C^T, respectively) compared to all available complete genomes of members of the *Nitrosopumilaceae* family. Strains NF5^T and D3C^T have a DNA base composition of 33.4 and 33.8 mol% G+C, respectively, which is within the range of other described *Nitrosopumilus* species (Table 1) and similar to members of the genus *Nitrosarchaeum* (~32.5 mol% G+C) [81, 82], '*Ca. Nitrosopelagicus brevis*' CN25 (33.2 mol% G+C) [23], and members of the provisional genus '*Nitrosocosmicus*' (~34.0 mol% G+C) [28, 29, 36]. It is lower than that of '*Ca. Nitrosotalea devanateri*' Nd1 (37.1 mol% G+C) [83], members of the provisional genus '*Nitrosotenuis*' (41.0–42.2 mol% G+C) [34, 35, 37], members of the genus *Nitrososphaera* (48.4–52.7 mol% G+C) [25, 26, 30] and '*Ca. Cenarchaeum symbiosum*' (57.4 mol% G+C) [84]. These results indicate that while DNA base composition is similar within members of the same genus, it can greatly differ between members of the same family in AOA (Fig. 4).

On the basis of phenotypic, genotypic and chemotaxonomic characteristics, strains NF5^T and D3C^T can be assigned to distinct species, *Nitrosopumilus adriaticus* sp. nov. and *Nitrosopumilus piranensis* sp. nov., respectively.

DESCRIPTION OF *NITROSOPUMILUS ADRIATICUS* SP. NOV.

Nitrosopumilus adriaticus (a.dri.a'ti.cus. L. masc. adj. *adriaticus* from the Adriatic Sea; describing the location the type strain was isolated).

Cells appear as small, regular, slender rods with a length of 0.59–1.74 µm and a diameter of 0.20–0.25 µm. Cells are occasionally flagellated. Cells tolerate ammonia and nitrite concentrations of up to 25 mM and 10 mM, respectively.

Urease-negative. Growth occurs between 15 and 34 °C, with an optimum of 30–32 °C. The pH range for growth is pH 6.8–8.0, with an optimum of pH 7.1. The salinity range for growth is 10–55 ‰, with an optimum of 34 ‰. The minimum generation time is approximately 34 h. Average ammonia oxidation and carbon fixation rates are 6.5 ± 3.2 and 0.69 ± 0.29 fmol cell⁻¹ d⁻¹, respectively. Cells have a C:N ratio of 3.91 and the cellular metal abundance ranking is Fe>Zn>Cu>Mn>Co.

The type strain is NF5^T (=JCM 32270^T =NCIMB 15114^T), isolated from coastal surface waters of the Northern Adriatic Sea, off the coast of Piran, Slovenia. The G+C content of the genomic DNA of the type strain is 33.4 mol%. The GenBank accession number for the 16S rRNA gene sequence of strain NF5^T is MK139955 and the genome is deposited under the accession number CP010868.

DESCRIPTION OF *NITROSOPUMILUS PIRANENSIS* SP. NOV.

Nitrosopumilus piranensis (pi.ran.en'sis. N.L. fem. adj. *piranensis* from the coast off Piran; describing the location the type strain was isolated).

Cells appear as small, regular, slender rods with a length of 0.49–2.00 µm and a diameter of 0.20–0.25 µm. Motility is not observed. Cells tolerate ammonia and nitrite concentrations of up to 30 mM and 15 mM, respectively. Urease-positive. Growth occurs between 15 and 37 °C, with an optimum of 32 °C. The pH range for growth is pH 6.8–8.0, with an optimum of pH 7.1–7.3. The salinity range for growth is 15–65 ‰, with an optimum of 37 ‰. The minimum generation time is approximately 27 h. Average ammonia oxidation and carbon fixation rates are 7.2 ± 3.7 and 0.64 ± 0.37 fmol cell⁻¹ d⁻¹, respectively. Cells have a C:N ratio of 3.98, containing approx. 16.3 fg C cell⁻¹ and 4.78 fg N cell⁻¹. The cellular metal abundance ranking is Fe>Zn>Cu>Mn>Co. Cells potentially store iron, exhibiting intracellular Fe:C quota of 519–622 µmol Fe per mol cell-C.

The type strain is D3C^T (=JCM 32271^T =DSM 106147^T =NCIMB 15115^T), isolated from coastal surface waters of the Northern Adriatic Sea, off the coast of Piran. The G+C content of the genomic DNA of the type strain is 33.8 mol%. The GenBank accession number for the 16S rRNA gene sequence of strain D3C^T is MK139956 and the genome is deposited under the accession number CP010868.

Funding information

The experimental work was supported by the Austrian Science Fund (FWF) project (P28781-B21) to G. J. H. B. B. was supported by the Uni-docs fellowship of the University of Vienna and the FWF DK+project 'Microbial Nitrogen Cycling' (project number W1257-B20).

Acknowledgements

We thank Romana Bittner and Christian Baranyi for technical assistance with cultivations, Meriel Bittner for occasional sampling, Herwig Lenitz for measuring metal concentrations and Hubert Kraill for C:N ratio measurements. We also thank Stephan Krämer and Logan

Hodgskiss for helpful comments. We are grateful to Martin Könneke and Felix Elling for providing detailed lipid composition data of both strains.

Conflict of interest

The authors declare that there are no conflicts of interest.

References

- Wuchter C, Abbas B, Coolen MJ, Herfort L, van Bleijswijk J, van BJ et al. Archaeal nitrification in the ocean. *Proc Natl Acad Sci USA* 2006;103:12317–12322.
- Leininger S, Urlich T, Schloter M, Schwark L, Qi J et al. Archaea predominate among ammonia-oxidizing prokaryotes in soils. *Nature* 2006;442:806–809.
- Karner MB, Delong EF, Karl DM. Archaeal dominance in the mesopelagic zone of the Pacific Ocean. *Nature* 2001;409:507–510.
- Teira E, Reinthaler T, Pernthaler A, Pernthaler J, Herndl GJ. Combining catalyzed reporter deposition-fluorescence in situ hybridization and microautoradiography to detect substrate utilization by bacteria and Archaea in the deep ocean. *Appl Environ Microbiol* 2004;70:4411–4414.
- Wuchter C, Schouten S, Boschker HT, Sinninghe Damsté JS. Bicarbonate uptake by marine Crenarchaeota. *FEMS Microbiol Lett* 2003;219:203–207.
- Könneke M, Bernhard AE, de La Torre JR, Walker CB, Waterbury JB et al. Isolation of an autotrophic ammonia-oxidizing marine archaeon. *Nature* 2005;437:543–546.
- Ingalls AE, Shah SR, Hansman RL, Aluwihare LI, Santos GM et al. Quantifying archaeal community autotrophy in the mesopelagic ocean using natural radiocarbon. *Proc Natl Acad Sci USA* 2006;103:6442–6447.
- Prosser JI, Nicol GW. Relative contributions of archaea and bacteria to aerobic ammonia oxidation in the environment. *Environ Microbiol* 2008;10:2931–2941.
- Martens-Habbena W, Berube PM, Urakawa H, de La Torre JR, Stahl DA. Ammonia oxidation kinetics determine niche separation of nitrifying archaea and bacteria. *Nature* 2009;461:976–979.
- Horak RE, Qin W, Schauer AJ, Armbrust EV, Ingalls AE et al. Ammonia oxidation kinetics and temperature sensitivity of a natural marine community dominated by archaea. *ISME J* 2013;7:2023–2033.
- Lam P, Kuypers MM. Microbial nitrogen cycling processes in oxygen minimum zones. *Ann Rev Mar Sci* 2011;3:317–345.
- Stewart FJ, Ulloa O, Delong EF. Microbial metatranscriptomics in a permanent marine oxygen minimum zone. *Environ Microbiol* 2012;14:23–40.
- Hawley AK, Brewer HM, Norbeck AD, Paša-Tolić L, Hallam SJ. Metaproteomics reveals differential modes of metabolic coupling among ubiquitous oxygen minimum zone microbes. *Proc Natl Acad Sci USA* 2014;111:11395–11400.
- Qin W, Meinhardt KA, Moffett JW, Devol AH, Virginia Armbrust E et al. Influence of oxygen availability on the activities of ammonia-oxidizing archaea. *Environ Microbiol Rep* 2017;9:250–256.
- Santoro AE, Buchwald C, McIlvin MR, Casciotti KL. Isotopic signature of N(2)O produced by marine ammonia-oxidizing archaea. *Science* 2011;333:1282–1285.
- Löscher CR, Kock A, Könneke M, Laroche J, Bange HW et al. Production of oceanic nitrous oxide by ammonia-oxidizing archaea. *Biogeosciences* 2012;9:2419–2429.
- Freig A, Wallace DW, Bange HW. Global oceanic production of nitrous oxide. *Philos Trans R Soc Lond B Biol Sci* 2012;367:1245–1255.
- Qin W, Heal KR, Ramdasi R, Kobelt JN, Martens-Habbena W et al. *Nitrosopumilus maritimus* gen. nov., sp. nov., *Nitrosopumilus cobalaminigenes* sp. nov., *Nitrosopumilus oxycliniae* sp. nov., and *Nitrosopumilus ureiphilus* sp. nov., four marine ammonia-oxidizing archaea of the phylum Thaumarchaeota. *Int J Syst Evol Microbiol* 2017;67:5067–5079.
- Bayer B, Vojvoda J, Offre P, Alves RJ, Elisabeth NH et al. Physiological and genomic characterization of two novel marine thaumarchaeal strains indicates niche differentiation. *ISME J* 2016;10:1051–1063.
- Park SJ, Ghai R, Martín-Cuadrado AB, Rodríguez-Valera F, Chung WH et al. Genomes of two new ammonia-oxidizing archaea enriched from deep marine sediments. *PLoS One* 2014;9:e96449.
- Mosier AC, Allen EE, Kim M, Ferriera S, Francis CA. Genome sequence of "Candidatus Nitrosopumilus salaria" BD31, an ammonia-oxidizing archaeon from the San Francisco Bay Estuary. *J Bacteriol* 2012;194:2121–2122.
- Mosier AC, Lund MB, Francis CA. Ecophysiology of an ammonia-oxidizing archaeon adapted to low-salinity habitats. *Microb Ecol* 2012;64:955–963.
- Santoro AE, Dupont CL, Richter RA, Craig MT, Carini P et al. Genomic and proteomic characterization of "Candidatus Nitrosopelagicus brevis": an ammonia-oxidizing archaeon from the open ocean. *Proc Natl Acad Sci USA* 2015;112:1173–1178.
- Ahlgren NA, Chen Y, Needham DM, Parada AE, Sachdeva R et al. Genome and epigenome of a novel marine Thaumarchaeota strain suggest viral infection, phosphorothioation DNA modification and multiple restriction systems. *Environ Microbiol* 2017;19:2434–2452.
- Tourna M, Stieglmeier M, Spang A, Könneke M, Schintlmeister A et al. *Nitrososphaera viennensis*, an ammonia oxidizing archaeon from soil. *Proc Natl Acad Sci USA* 2011;108:8420–8425.
- Zhalnina KV, Dias R, Leonard MT, Dorr de Quadros P, Camargo FA et al. Genome sequence of *Candidatus Nitrososphaera evergladensis* from group I.1b enriched from Everglades soil reveals novel genomic features of the ammonia-oxidizing archaea. *PLoS One* 2014;9:e101648.
- Jung MY, Park SJ, Kim SJ, Kim JG, Sinninghe Damsté JS et al. A mesophilic, autotrophic, ammonia-oxidizing archaeon of thaumarchaeal group I.1a cultivated from a deep oligotrophic soil horizon. *Appl Environ Microbiol* 2014;80:3645–3655.
- Lehtovirta-Morley LE, Ross J, Hink L, Weber EB, Gubry-Rangin C et al. Isolation of "Candidatus Nitrosocosmicus franklandus", a novel ureolytic soil archaeal ammonia oxidiser with tolerance to high ammonia concentration. *FEMS Microbiol Ecol* 2016;92:fiw057–10.
- Jung MY, Kim JG, Sinninghe Damsté JS, Rijpstra WI, Madsen EL et al. A hydrophobic ammonia-oxidizing archaeon of the *Nitrosocosmicus* clade isolated from coal tar-contaminated sediment. *Environ Microbiol Rep* 2016;8:983–992.
- Spang A, Poehlein A, Offre P, Zumbärgel S, Haider S et al. The genome of the ammonia-oxidizing *Candidatus Nitrososphaera gargensis*: insights into metabolic versatility and environmental adaptations. *Environ Microbiol* 2012;14:3122–3145.
- Abby SS, Melcher M, Kerou M, Krupovic M, Stieglmeier M et al. *Candidatus Nitrosocaldus cavascurensis*, an ammonia oxidizing, extremely thermophilic archaeon with a highly mobile genome. *Front Microbiol* 2018;9:28.
- Daebeler A, Herbold CW, Vierheilig J, Sedlacek CJ, Pjevac P et al. Cultivation and genomic analysis of "Candidatus Nitrosocaldus islandicus," an obligately thermophilic, ammonia-oxidizing Thaumarchaeon from a hot Spring biofilm in Graendalur Valley, Iceland. *Front Microbiol* 2018;9:193.
- de La Torre JR, Walker CB, Ingalls AE, Könneke M, Stahl DA. Cultivation of a thermophilic ammonia oxidizing archaeon synthesizing crenarchaeol. *Environ Microbiol* 2008;10:810–818.
- Lebedeva EV, Hatzepichler R, Pelletier E, Schuster N, Hauzmayer S et al. Enrichment and genome sequence of the group I.1a ammonia-oxidizing archaeon "Ca. Nitrosotenuis uzonensis" representing a clade globally distributed in thermal habitats. *PLoS One* 2013;8:e80835.
- Li Y, Ding K, Wen X, Zhang B, Shen B et al. A novel ammonia-oxidizing archaeon from wastewater treatment plant: Its enrichment, physiological and genomic characteristics. *Sci Rep* 2016;6:23747.

36. Sauder LA, Albertsen M, Engel K, Schwarz J, Nielsen PH et al. Cultivation and characterization of *Candidatus Nitrosocosmicus exaquare*, an ammonia-oxidizing archaeon from a municipal wastewater treatment system. *ISME J* 2017;11:1142–1157.
37. Sauder LA, Engel K, Lo C-C CP, Neufeld JD. Cultivation and characterization of *Candidatus Nitrosotenuis aquariensis*, an ammonia-oxidizing archaeon from a freshwater aquarium biofilter. *Appl Environ Microbiol* 2018;AEM.01430-18.
38. Qin W, Amin SA, Martens-Habbena W, Walker CB, Urakawa H et al. Marine ammonia-oxidizing archaeal isolates display obligate mixotrophy and wide ecotypic variation. *Proc Natl Acad Sci USA* 2014;111:12504–12509.
39. Carini P, Dupont CL, Santoro AE. Patterns of thaumarchaeal gene expression in culture and diverse marine environments. *Environ Microbiol* 2018;20:2112–2124.
40. Palatinszky M, Herbold C, Jehmlich N, Pogoda M, Han P et al. Cyanate as an energy source for nitrifiers. *Nature* 2015;524:105–108.
41. Kim JG, Park SJ, Sinninghe Damsté JS, Schouten S, Rijpsma WI et al. Hydrogen peroxide detoxification is a key mechanism for growth of ammonia-oxidizing archaea. *Proc Natl Acad Sci USA* 2016;113:7888–7893.
42. Heal KR, Qin W, Ribault F, Bertagnolli AD, Coyote-Maestas W et al. Two distinct pools of B12 analogs reveal community interdependencies in the ocean. *Proc Natl Acad Sci USA* 2017;114:364–369.
43. Walker CB, de La Torre JR, Klotz MG, Urakawa H, Pinel N et al. *Nitrosopumilus maritimus* genome reveals unique mechanisms for nitrification and autotrophy in globally distributed marine crenarchaea. *Proc Natl Acad Sci USA* 2010;107:8818–8823.
44. Stieglmeier M, Klingl A, Alves RJ, Rittmann SK, Melcher M et al. *Nitrososphaera viennensis* gen. nov., sp. nov., an aerobic and mesophilic, ammonia-oxidizing archaeon from soil and a member of the archaeal phylum Thaumarchaeota. *Int J Syst Evol Microbiol* 2014;64:2738–2752.
45. Holmes RM, Aminot A, Kérouel R, Hooker BA, Peterson BJ. A simple and precise method for measuring ammonium in marine and freshwater ecosystems. *Can J Fish Aquat Sci* 1999;56:1801–1808.
46. Griess P. Bemerkungen zu der Abhandlung der HH. Weselsky und Benedikt "Über einige Azoverbindungen". *Chem Ber* 1879;12:426–428.
47. Marie D, Brussaard CPD, Thyrhaug R, Bratbak G, Vaulot D. Enumeration of marine viruses in culture and natural samples by flow cytometry. *Appl Environ Microbiol* 1999;65:45–52.
48. Herndl GJ, Reinthaler T, Teira E, van Aken H, Veth C et al. Contribution of archaea to total prokaryotic production in the deep Atlantic Ocean. *Appl Environ Microbiol* 2005;71:2303–2309.
49. Tovar-Sanchez A, Sañudo-Wilhelmy SA, Garcia-Vargas M, Weaver RS, Popels LC et al. A trace metal clean reagent to remove surface-bound iron from marine phytoplankton. *Mar Chem* 2003;82:91–99.
50. Anderegg G, Arnaud-Neu F, Delgado R, Felcman J, Popov K. Critical evaluation of stability constants of metal complexes of complexones for biomedical and environmental applications* (IUPAC Technical Report). *Pure and Applied Chemistry* 2005;77:1445–1495.
51. Elling FJ, Könneke M, Nicol GW, Stieglmeier M, Bayer B et al. Chemotaxonomic characterisation of the thaumarchaeal lipidome. *Environ Microbiol* 2017;19:2681–2700.
52. Katoh K, Standley DM. MAFFT multiple sequence alignment software version 7: improvements in performance and usability. *Mol Biol Evol* 2013;30:772–780.
53. Criscuolo A, Gribaldo S, Bmge GS. BMGE (Block Mapping and Gathering with Entropy): a new software for selection of phylogenetic informative regions from multiple sequence alignments. *BMC Evol Biol* 2010;10:210.
54. Nguyen LT, Schmidt HA, von Haeseler A, Minh BQ. IQ-TREE: a fast and effective stochastic algorithm for estimating maximum-likelihood phylogenies. *Mol Biol Evol* 2015;32:268–274.
55. Martens-Habbena W, Berube PM, Urakawa H, de La Torre JR, Stahl DA. Ammonia oxidation kinetics determine niche separation of nitrifying archaea and bacteria. *Nature* 2009;461:976–979.
56. Peng X, Fuchsman CA, Jayakumar A, Oleynik S, Martens-Habbena W et al. Ammonia and nitrite oxidation in the Eastern Tropical North Pacific. *Global Biogeochem Cycles* 2015;29:2034–2049.
57. Santoro AE, Casciotti KL, Francis CA. abundance and diversity of nitrifying archaea. *Environ Microbiol* 2010;12:1989–2006.
58. Varela MM, van Aken HM, Sintès E, Reinthaler T, Herndl GJ. Contribution of Crenarchaeota and Bacteria to autotrophy in the North Atlantic interior. *Environ Microbiol* 2011;13:1524–1533.
59. Clark DR, Rees AP, Joint I. Ammonium regeneration and nitrification rates in the oligotrophic Atlantic Ocean: Implications for new production estimates. *Limnol Oceanogr* 2008;53:52–62.
60. Francis CA, Roberts KJ, Beman JM, Santoro AE, Oakley BB. Ubiquity and diversity of ammonia-oxidizing archaea in water columns and sediments of the ocean. *Proc Natl Acad Sci USA* 2005;102:14683–14688.
61. Glover HE. The relationship between inorganic nitrogen oxidation and organic carbon production in batch and chemostat cultures of marine nitrifying bacteria. *Arch Microbiol* 1985;142:45–50.
62. Könneke M, Schubert DM, Brown PC, Hügler M, Standfest S et al. Ammonia-oxidizing archaea use the most energy-efficient aerobic pathway for CO₂ fixation. *Proc Natl Acad Sci USA* 2014;111:8239–8244.
63. Kozłowski JA, Stieglmeier M, Schleper C, Klotz MG, Stein LY. Pathways and key intermediates required for obligate aerobic ammonia-dependent chemolithotrophy in bacteria and *Thaumarchaeota*. *ISME J* 2016;10:1836–1845.
64. Yan J, Haaïjer SC, Op den Camp HJ, van Niftrik L, Stahl DA et al. Mimicking the oxygen minimum zones: stimulating interaction of aerobic archaeal and anaerobic bacterial ammonia oxidizers in a laboratory-scale model system. *Environ Microbiol* 2012;14:3146–3158.
65. Martens-Habbena W, Qin W, Horak RE, Urakawa H, Schauer AJ et al. The production of nitric oxide by marine ammonia-oxidizing archaea and inhibition of archaeal ammonia oxidation by a nitric oxide scavenger. *Environ Microbiol* 2015;17:2261–2274.
66. Srithep P, Pornkulwat P, Limpiyakorn T. Contribution of ammonia-oxidizing archaea and ammonia-oxidizing bacteria to ammonia oxidation in two nitrifying reactors. *Environ Sci Pollut Res Int* 2018;25:8676–8687.
67. Jung MY, Well R, Min D, Giesemann A, Park SJ et al. Isotopic signatures of N₂O produced by ammonia-oxidizing archaea from soils. *ISME J* 2014;8:1115–1125.
68. Offre P, Kerou M, Spang A, Schleper C. Variability of the transporter gene complement in ammonia-oxidizing archaea. *Trends Microbiol* 2014;22:665–675.
69. Ouverney CC, Fuhrman JA. Marine planktonic archaea take up amino acids. *Appl Environ Microbiol* 2000;66:4829–4833.
70. Björkman KM, Church MJ, Doggett JK, Karl DM. Differential assimilation of inorganic carbon and leucine by *Prochlorococcus* in the oligotrophic North Pacific subtropical gyre. *Front Microbiol* 2015;6:1401.
71. Cunningham BR, John SG. The effect of iron limitation on cyanobacteria major nutrient and trace element stoichiometry. *Limnol Oceanogr* 2017;62:846–858.
72. Coleman JE. Zinc proteins: enzymes, storage proteins, transcription factors, and replication proteins. *Annu Rev Biochem* 1992;61:897–946.
73. Amin SA, Moffett JW, Martens-Habbena W, Jacquot JE, Han Y et al. Copper requirements of the ammonia-oxidizing archaeon *Nitrosopumilus maritimus* SCM1 and implications for nitrification in the marine environment. *Limnol Oceanogr* 2013;58:2037–2045.

74. Smith JM, Chavez FP, Francis CA. Ammonium uptake by phytoplankton regulates nitrification in the sunlit ocean. *PLoS One* 2014; 9:e108173.
75. Horak REA, Qin W, Bertagnolli AD, Nelson A, Heal KR *et al.* Relative impacts of light, temperature, and reactive oxygen on thaumarchaeal ammonia oxidation in the North Pacific Ocean. *Limnol Oceanogr* 2018;63:741–757.
76. Tolar BB, Powers LC, Miller WL, Wallsgrove NJ, Popp BN *et al.* Ammonia oxidation in the ocean can be inhibited by nanomolar concentrations of hydrogen peroxide. *Front Mar Sci* 2016;3:237.
77. Jarrell KF, Ding Y, Nair DB, Siu S. Surface appendages of archaea: structure, function, genetics and assembly. *Life* 2013;3:86–117.
78. Elling FJ, Becker KW, Könneke M, Schröder JM, Kellermann MY *et al.* Respiratory quinones in archaea: phylogenetic distribution and application as biomarkers in the marine environment. *Environ Microbiol* 2016;18:692–707.
79. Brochier-Armanet C, Boussau B, Gribaldo S, Forterre P. Mesophilic crenarchaeota: proposal for a third archaeal phylum, the Thaumarchaeota. *Nat Rev Microbiol* 2008;6:245–252.
80. Parks DH, Chuvpochina M, Waite DW, Rinke C, Skarszewski A *et al.* A proposal for a standardized bacterial taxonomy based on genome phylogeny. *Nat Biotechnol* 2018;36:996–1004.
81. Blainey PC, Mosier AC, Potanina A, Francis CA, Quake SR. Genome of a low-salinity ammonia-oxidizing archaeon determined by single-cell and metagenomic analysis. *PLoS One* 2011;6: e16626.
82. Jung MY, Islam MA, Gwak JH, Kim JG, Rhee SK. *Nitrosarchaeum koreense* gen. nov., sp. nov., an aerobic and mesophilic, ammonia-oxidizing archaeon member of the phylum Thaumarchaeota isolated from agricultural soil. *Int J Syst Evol Microbiol* 2018;68: 3084–3095.
83. Lehtovirta-Morley LE, Sayavedra-Soto LA, Gallois N, Schouten S, Stein LY *et al.* Identifying potential mechanisms enabling acidophily in the ammonia-oxidizing archaeon "*Candidatus Nitrosotalea devanaterrea*". *Appl Environ Microbiol* 2016;82:2608–2619.
84. Hallam SJ, Konstantinidis KT, Putnam N, Schleper C, Watanabe Y *et al.* Genomic analysis of the uncultivated marine crenarchaeote *Cenarchaeum symbiosum*. *Proc Natl Acad Sci USA* 2006;103: 18296–18301.

Five reasons to publish your next article with a Microbiology Society journal

1. The Microbiology Society is a not-for-profit organization.
2. We offer fast and rigorous peer review – average time to first decision is 4–6 weeks.
3. Our journals have a global readership with subscriptions held in research institutions around the world.
4. 80% of our authors rate our submission process as 'excellent' or 'very good'.
5. Your article will be published on an interactive journal platform with advanced metrics.

Find out more and submit your article at microbiologyresearch.org.